



HAL
open science

Non data aided timing recovery algorithms for digital underwater acoustic communications

Goulven Eynard, Christophe Laot

► **To cite this version:**

Goulven Eynard, Christophe Laot. Non data aided timing recovery algorithms for digital underwater acoustic communications. OCEANS'07, June 18-21, Aberdeen, Scotland, Jun 2008, Aberdeen, United Kingdom. hal-02121159

HAL Id: hal-02121159

<https://hal.science/hal-02121159>

Submitted on 6 May 2019

HAL is a multi-disciplinary open access archive for the deposit and dissemination of scientific research documents, whether they are published or not. The documents may come from teaching and research institutions in France or abroad, or from public or private research centers.

L'archive ouverte pluridisciplinaire **HAL**, est destinée au dépôt et à la diffusion de documents scientifiques de niveau recherche, publiés ou non, émanant des établissements d'enseignement et de recherche français ou étrangers, des laboratoires publics ou privés.

Non Data Aided Timing Recovery Algorithm for Digital Underwater Communications

Goulven Eynard and Christophe Laot

GET, ENST Bretagne Signal and Communication department, CNRS TAMCIC,
Technopole Brest-Iroise - CS 83818 - 29238 Brest Cedex 3, France
Email: {Goulven.Eynard, Christophe.Laot}@enst-bretagne.fr

Abstract—Synchronization is a critical operation in an underwater acoustic data communication receiver. This paper proposes a comparison of two digital NDA (non data aided) timing recovery schemes, referenced in literature as the Gardner, and the Oerder and Meyr algorithms. We consider the context of a single QPSK carrier continuous transmission, where a timing shift has to be estimated continuously in order to track the optimum sample time. Simulations processed on real data taken from sea trials, collected by the GESMA in collaboration with SERCEL and ENST Bretagne, reveal that a large Doppler shift or a large jitter on the timing shift estimation can introduce cycle slips in the clock synchronizer, which generate a large burst of errors in the data receiver. These perturbations can dramatically affect the global performance of the transmission system.

I. INTRODUCTION

Synchronization is a critical operation in an underwater acoustic data communication receiver. In fact, without a sufficiently accurate knowledge of the synchronization parameters, the task of retrieving the symbol sequence from the received signal can be highly time and power consuming for the receiver. This is particularly the case in a digital underwater acoustic link, where the channel can be subject to severe time-space variability, strong multipath and Doppler effect that make the estimation of the synchronization parameters very difficult in practice. The particular case of the Doppler carrier phase tracking with Doppler compensation is relevant and is well explored in [7] and [8].

This paper addresses the problem of NDA (Non Data Aided) timing recovery. Timing recovery is often the first synchronization operation processed by the digital receiver and so is a vital part of any synchronous receiver. We consider the context of a single carrier QPSK continuous transmission, where a timing shift has to be estimated continuously in order to track the optimum sample time. We also suppose that the received signal is sampled at a frequency sufficiently high so that interpolation is not necessary. The first recovery scheme is an error-tracking synchronizer, based on the tracking of the average zero-crossing instant of the received signal using a digital locked loop (DLL). The fact that this adaptive algorithm provides an estimation of the timing shift each symbol time allows a high sensitivity to strong variations of the timing estimate. On the other hand, the feedback structure can introduce cycle-slips and hang-up problems [5].

The second recovery scheme, commonly referred as the Oerder and Meyr algorithm, uses the cyclostationary property of the

received signal to recover the timing shift. This algorithm uses a feedforward structure: the timing error estimation is processed directly from the received signal sampled at a constant frequency. This type of algorithm is particularly adapted in short burst mode, where it is sufficient to make a single estimation for each burst of data. We consider here the situation of a continuous transmission: we divide the received data into blocks of length L symbols and we successively estimate the timing shift for each block. In order to track variations of the timing shift caused for instance by a relative motion between the emitter and the receiver, the successive estimates have to be unwrapped by means of a post-processing structure [2], [5], [6]. This algorithm supposes that the timing shift has no variation during the transmission of an observation interval. The major drawback of this algorithm comes from variations of the timing shift that are not taken into account. The main contribution of this paper is the study of these two timing recovery algorithms applied to the digital underwater transmission context. We observe that a large Doppler shift or a large jitter on the timing shift estimation can introduce the deletion of symbols in the clock synchronizer, generating large bursts of errors. This perturbation, known in literature as a cycle slip, can dramatically affect the global performance of the transmission system.

The paper is organized as follows. In Section II the baseband model is introduced. We present successively in Section III the Gardner algorithm, and in Section IV the Oerder and Meyr algorithm. In Section V, the two algorithms adapted to the single input, multiple output context is presented. Finally, the performance of the two algorithms are compared using data from sea trials in Section VI.

II. BASEBAND MODEL

We consider the timing recovery for digital data transmission with linear modulation schemes. The received, filtered and sampled baseband signal from the input channel can be written as:

$$r(kT_e) = \sum_{n=-\infty}^{+\infty} a_n g(kT_e - nT_s - \tau[k]T_e) + w(kT_e), \quad (1)$$

where the transmitted symbols are represented by $\{a_n\}$ (QPSK modulation) and assumed to be mutually uncorrelated. $g(t)$ includes the transmitting and the receiving filter of the communication system as well as the channel impulse response. T_e

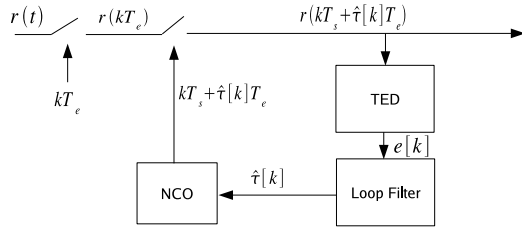


Fig. 1: The feedback structure (digital locked loop)

denotes the sampling period. Let T_s be the symbol duration. We suppose that $T_s = NT_e$, where N is the oversampling factor. In the specific case of an underwater acoustic communication, the relatively low data rate allows us to take a large value for the oversampling factor N , so that no interpolation is necessary. $\tau[k]$ is the unknown varying timing shift. $w(t)$ is the channel noise which is assumed to be white and gaussian. First, the digital receiver operates the timing recovery. Then, data are estimated with the SA-DFE (self adaptive decision feedback equalizer), which is presented in [3] for the SISO (single input, single output) case, and in [4] and [9] for the SIMO (single input, multiple output) case.

III. GARDNER TIMING RECOVERY ALGORITHM

At the heart of the feedback structure (or digital locked loop) is a TED (timing error detector), which serves to extract timing error information from the received signal. The error signal $e[k]$ at the output of the TED is filtered through the loop filter. When the DLL is in lock, $e[k]$ is nearly proportionnal to the difference between $\tau[k]$ and the timing estimate $\hat{\tau}[k]$. The NCO (numerical controlled oscillator) tends to lock the local clock onto the incoming signal using the timing error information provided by the loop filter. The Gardner TED [1] uses the zero-crossing instant of the received signal as an information to perform timing-recovery. Defining:

$$T[k] = kT_s + \hat{\tau}[k]T_e,$$

the output of the Gardner timing error detector can be expressed as:

$$e[k] = \Re \left\{ \left[r(T[k-1]) - r(T[k]) \right] r^* \left(T[k] - T_s/2 \right) \right\}. \quad (2)$$

The error signal is then filtered through a first-order filter loop. The transfert function loop filter employed here is:

$$F(z) = \frac{1 - \lambda}{1 - \lambda z^{-1}}, \quad (3)$$

where the forgetting factor λ is taken at the value: $\lambda = 0.99$. This factor has been chosen as the best heuristic trade-off between the acquisition time and the filtering of the noise. The NCO provides at its output the corrected sampling signal. Further details of this algorithm can be found in [1].

IV. OERDER AND MEYR ALGORITHM

A. Feedforward Structure

The main difference of the feedforward structure compared to the feedback structure is that the estimation of the timing error is obtained directly from the received signal $r(t)$ sampled at a constant frequency $f_e = 1/T_e$, with $T_s = NT_e$. No information previously computed is used when the sampling operation is processed. Also we call L the length of the observation interval in symbol periods and $\mathbf{r}[m] = \{r(kT_e)\}_{mLN \leq k \leq (m+1)LN-1}$ the observation interval itself. We note that each observation interval $\mathbf{r}[m]$ is composed of NL samples.

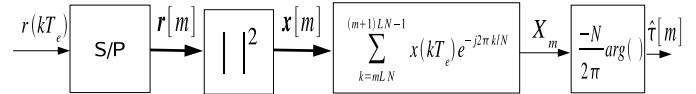


Fig. 2: Block diagram of the Oerder and Meyr estimator

The squared sequence of the observation interval contains a spectral component at $1/T_s$ that can be used for the estimation of the parameter τ :

$$\mathbf{x}[m] = \{x(kT_e)\}_{mLN \leq k \leq (m+1)LN-1}, \quad (4)$$

where

$$x(kT_e) = \left| r(kT_e) \right|^2.$$

The spectral component is extracted by computing the complex Fourier coefficient:

$$X_m = \sum_{k=mLN}^{(m+1)LN-1} x(kT_e) e^{-j2\pi k/N}. \quad (5)$$

The argument of the Fourier transform gives the modulo N of the timing estimate within a factor $-N/2\pi$:

$$\hat{\tau}[m] = -N/2\pi \text{Arg}(X_m). \quad (6)$$

Further details can be found in [2] about this estimator.

Successive estimations are needed to track fluctuations of the synchronization parameter. Feedforward estimation involves dividing the received signal into observation intervals that are short enough to make the approximation that the timing shift is constant. We notice that the resulting feedforward estimates at the output of the Oerder and Meyr estimator (Figure 3) are restricted to the basic interval: $-N \leq \hat{\tau}[m] \leq N$. In fact, the feedforward estimates can be considered as estimates of the synchronization parameters reduced modulo the interval $[-N; N]$. We want to remove this modulo N operation to track the timing shift $\tau[m]$. This problem is solved by unwrapping the feedforward estimates.

B. Unwrapping Algorithm

In this section, we give details on how to accomplish the unwrapping operation. Let $SAW_N(x)$ be the sawtooth function with period N , defined on the interval $-\frac{N}{2} \leq x \leq \frac{N}{2}$ as:

$$SAW_N(\tilde{\Delta}_\tau[m]) = \tilde{\Delta}_\tau[m] \text{ if } |\tilde{\Delta}_\tau[m]| \leq \left| \frac{N}{2} \right|. \quad (7)$$

The sawtooth function is a useful function to unwrap the data. Having a look on Figure 3, we notice that the expression of the sawtooth function can be expressed from the modulo N function: $SAW_N(\tilde{\Delta}_\tau[m]) =$

$$\begin{cases} MOD_N(\tilde{\Delta}_\tau[m]) & \text{if } MOD_N(\tilde{\Delta}_\tau[m]) \leq N/2, \\ MOD_N(\tilde{\Delta}_\tau[m]) - N & \text{else.} \end{cases} \quad (8)$$

A more useful expression is given by the equation:

$$SAW_N(\tilde{\Delta}_\tau[m]) = MOD_N(\tilde{\Delta}_\tau[m] - N/2) - N/2. \quad (9)$$

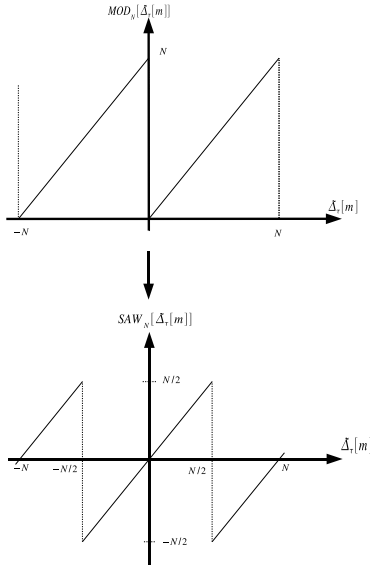


Fig. 3: Plot of the Modulo and the Sawtooth functions, supposing N the period of the two functions.

Having expressed the sawtooth function, we are now able to express $\hat{\tau}[m]$, supposing the knowledge of only $\hat{\tau}[m-1]$ and $\hat{\tau}[m]$.

Let $\Delta_\tau[m] = \hat{\tau}[m] - \hat{\tau}[m-1]$. We have:

$$\hat{\tau}[m] = \hat{\tau}[m-1] + \Delta_\tau[m].$$

Let $\tilde{\Delta}_\tau[m] = \hat{\tau}[m] - \hat{\tau}[m-1]$. Using the expression of $SAW_N(\tilde{\Delta}_\tau[m])$, it can be proven that:

$$\Delta_\tau[m] = SAW_N(\tilde{\Delta}_\tau[m]). \quad (10)$$

The expression of $\hat{\tau}[m]$ is finally obtained:

$$\hat{\tau}[m] = \hat{\tau}[m-1] + SAW_N(\tilde{\Delta}_\tau[m]), \quad (11)$$

which is illustrated by the unwrapping structure of Figure 4.

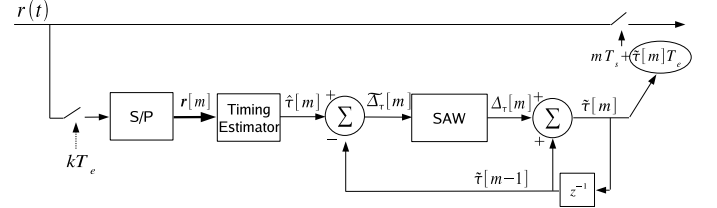


Fig. 4: The feedforward timing estimator with the unwrapping structure

V. SINGLE INPUT MULTIPLE OUTPUT TIMING RECOVERY

To exploit spatial diversity, timing estimation is processed on M channels independantly for both algorithms. Then, an average of the M timing estimates is used for sampling synchronously the M sensors. Figure 5 and 6 describe the timing recovery schemes for respectively the Oerder and Meyer and for the Gardner algorithm.

VI. COMPARISON OF THE ALGORITHMS ON REAL DATA

The evaluation of timing recovery algorithms is performed from the database collected by the GESMA in collaboration with SERCEL and ENST Bretagne during series of trials in the Atlantic ocean. At the receiver, the signal is demodulated using a free running oscillator. Then, timing recovery is processed on the baseband signal. Since the data rate is relatively low, we are able to choose an oversampling factor N sufficiently high so that interpolation is not necessary. Then, we jointly process equalization and phase synchronization using the unsupervised SA-DFE (Self-Adaptive Decision Feedback Equalizer), presented in [3] and [4] for the multi-sensors case. To exploit spatial diversity, $M = 4$ sensors are used at the receiver. For each simulation, we plot the evolution of the timing shift for both timing algorithms and of the estimated Mean Square Error (MSE) of the signal observed after the SA-DFE equalizer. Let the estimated MSE be:

$$e_MSE[k] = \beta e_MSE[k-1] + (1-\beta) \left| \hat{d}[k] - y[k] \right|^2, \quad (12)$$

where $\beta = 0.99$, $y[k]$ is the output of the SA-DFE equalizer and $\hat{d}[k]$ is the decision made on the estimated symbol $y[k]$. The estimated timing shift gives a reliable information on the Doppler shift present on the transmission. Also, it provides information on the jitter of the timing shift, due for instance to ISI (Intersymbol Interference) present on the channel. Moreover, a cycle slip is particularly recognizable in the evolution of the timing shift as a jump of length $\geq T_s$, where T_s is the symbol duration. The estimated MSE provides good indications on the performance of the global transmission system and on channel time-variations.

We first consider the case of a communication between an AUV (Autonomous Underwater Vehicle) and its surface base

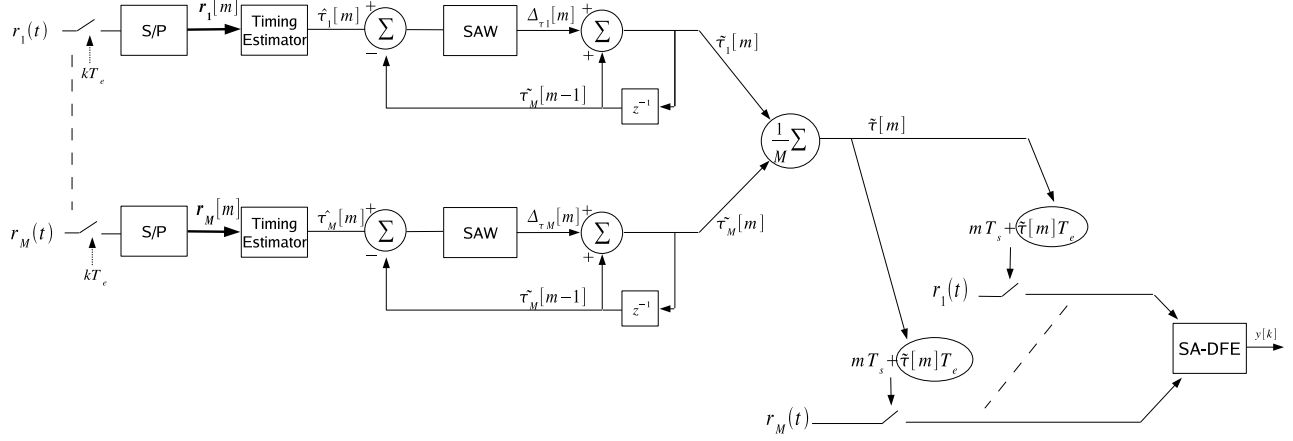


Fig. 5: Single Input - Multiple Output timing recovery scheme for the Oerder and Meyr Algorithm.

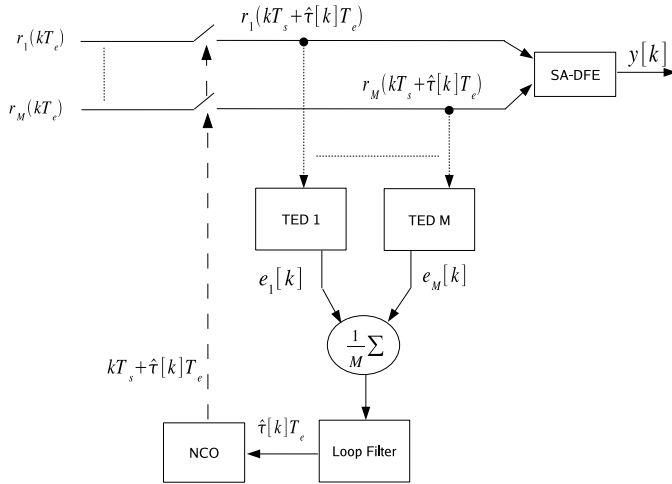


Fig. 6: Single Input - Multiple Output timing recovery scheme for the Gardner Algorithm.

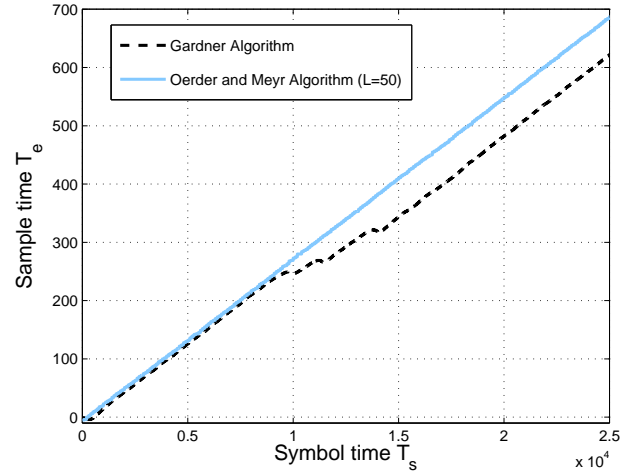


Fig. 7: Comparison of the evolution of the timing shift in time for the Oerder and Meyr, and the Gardner Algorithm.

station. The relative motion between the emitting and the receiving structures introduces a Doppler shift that can affect severely the tracking of the timing estimation. The transmission rate is $14kbp/s$, the modulation type is QPSK with carrier frequency at 35 kHz . At the receiver, the signal is sampled at $T_e = T_s/N$, where $T_s = 1.4 \cdot 10^{-4}s$ and $N = 20$.

We observe in Figure 8 that the Doppler shift is very large on this transmission ($800T_e = 40T_s$ over 30000 transmitted symbols: the Doppler shift in timing recovery is 0.13% of the symbol rate). It can be seen from Figure 8, that the large Doppler shift present on this channel causes two consecutive cycle slips in a relative small period of time (approximately $500T_s$) when Gardner algorithm is used. Both cycle slips have an immediate impact on the estimated MSE of the signal observed after the SA-DFE equalizer, as depicted in Figure 8. We choose $L = 50$ so that the Oerder and Meyr algorithm can track the fast evolutions of the timing shift. A larger value for L can be chosen: in [2], it is recommended to choose the length of the observation interval so that the variation of the

timing shift $\tau[m]$ is smaller than $T_s/2$. Hence, for a Doppler of $0, 13\%$, we can take a maximum value $L = 375$. However, to have a reliable continuous evaluation of the timing shift present on the channel and to face for example a brutal burst of noise, a heuristic value for the maximum variation of the timing shift on the observation interval could be $T_s/4$ or $T_s/8$. Therefore, the best value for L would be between 50 and 100 for this transmission.

We now consider the case of a static communication between the emitter and the receiver structure. The transmission rate is $8.75kbp/s$, the modulation type is QPSK with carrier frequency at 35 kHz . At the receiver, the signal is sampled at $T_e = T_s/32$, where $T_s = 2.2 \cdot 10^{-4}s$.

During the transmission, a strong impulsive noise occurs. We choose various values for parameter L ($L = 30, 50$) in order to erase this impulsive noise. As far as the length L of the observation interval is sufficient, we observe that the jitter of the timing-shift is considerably reduced. This observation is

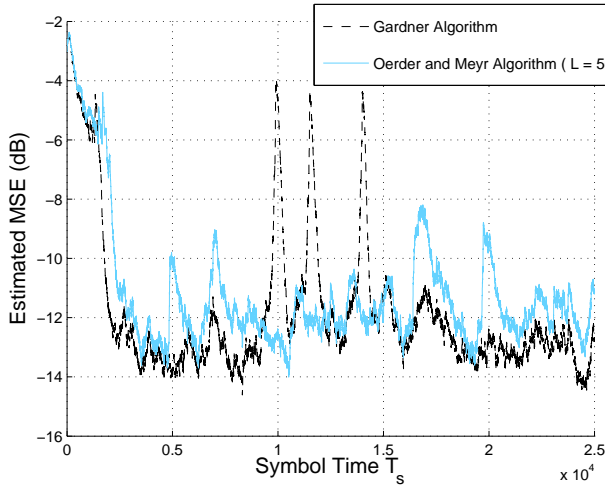


Fig. 8: Estimated MSE for the Oerder and Meyr and the Gardner Algorithm.

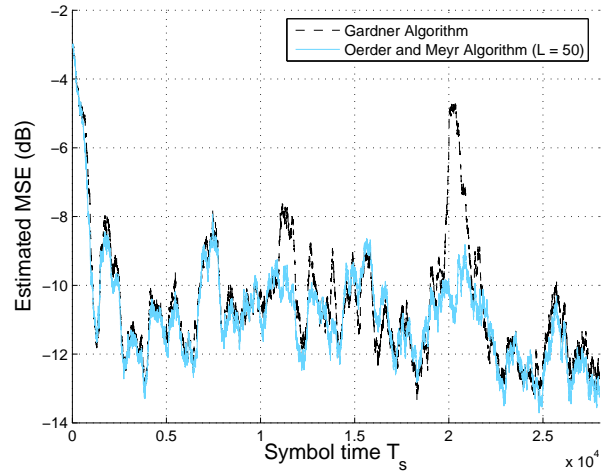


Fig. 10: Estimated MSE for the Oerder and Meyr and the Gardner Algorithm.

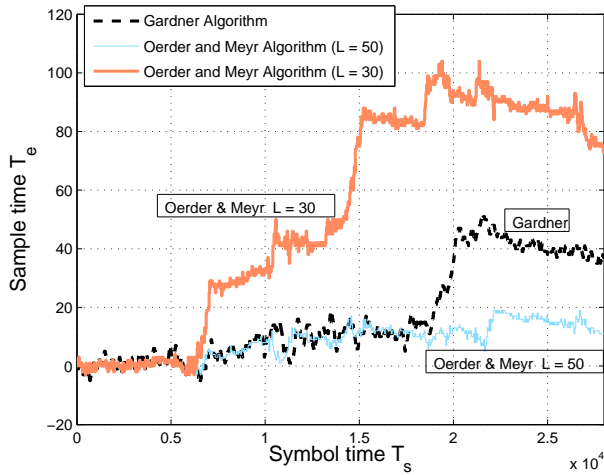


Fig. 9: Comparison of the evolution of the timing shift in time for the Oerder and Meyr, and the Gardner Algorithm.

confirmed by the result in [2], where it is shown that the mean square error of the estimate $\hat{\tau}[m]$ is inversely proportionnal to the parameter L when L is large. For the clarity of Figure 9 and 10, results obtained for $L > 50$ are not reported, since the performance are essentially the same as for $L = 50$. However, we notice that results obtained with $L = 30$ are far worse than results obtained with the Gardner algorithm. This can be explained by the fact that the effect of the impulsive noise can be attenuated if the observation interval is sufficiently large. Concerning the Gardner algorithm, we observe that the cycle-slip cannot be avoided by modifying the parameter of the loop filter λ . The cycle-slip in the tracking of the timing estimate is immediately repercutated in the estimated MSE of the SA-DFE in Figure 10.

Results obtained in these two examples show that the second algorithm is particularly well-fitted to underwater acoustic

communications if the parameter L is well chosen.

VII. CONCLUSION

The comparison of two well-known timing recovery algorithm is described here. A particular focus has been made on the unwrapping technique. Simulation on real data reveals that the Oerder and Meyr algorithm with a parameter L well chosen is more robust to cycles slips due to severe Doppler shift and burst of noise than the Gardner algorithm. The two transmissions reveal also that it exists a trade-off for the value of L where the Oerder and Meyr algorithm is able to face whether a large Doppler spread or a large burst of noise. Simulations conducted on various situations reveal that the value $L = 50$ or $L = 100$ appears to be a good trade off in our case to face large frequency offset and impulsive noise.

REFERENCES

- [1] F. Gardner, "A BPSK/QPSK Timing-Error Detector for Sampled Receivers," *IEEE Trans. Commun.*, vol. COM-34, pp. 423-429, May 1986.
- [2] M. Oerder and H. Meyr, "Digital Filter and Square Timing Recovery," *IEEE Trans. Commun.*, vol. COM-36, pp. 605-612, May 1988.
- [3] J. Labat, O. Macchi and C. Laot, "Adaptive Decision Feedback Equalization: Can You Skip The Training Period ?," *IEEE Trans. Commun.*, pp. 921-930, vol. 46, no. 7, July 1998.
- [4] J. Labat, C. Laot, "Blind adaptive Multiple-Input Decision Feedback Equalizer with a Self-Optimized Configuration," *IEEE Trans. Commun.*, vol. 49, pp.646-654, April 2001.
- [5] H. Meyr, M. Moeneclaey, and S. A. Fechtel, *Digital Communication Receivers: Synchronization, Channel Estimation, and Signal Processing*. New York: Wiley, 1998.
- [6] U. Mengali and A. N. D'Andrea, *Synchronization Techniques for Digital Receivers*. New York: Plenum, 1997.
- [7] L. Freitag, M. Johnson and M. Stojanovic, *Efficient Equalizer Update Algorithms for Acoustic Communication Channels of Varying complexity*. in *Proc. Ocean 97*, Oct 1997, pp. 580-585.
- [8] M. Johnson, L. Freitag and M. Stojanovic, *Improved Doppler Tracking and Correction for Underwater Acoustic Communications*. in *Proc. ICASSP 97*, Munich, Germany.
- [9] J. Trubuil, G. Lapierre, J. Labat, N. Beuzeulin, A. Goalic, C. Laot, *Improved AUV autonomy provided by an underwater acoustic link.*, in *Proc. ISOPE 2006*, San Francisco, USA.